Savannah River National Laboratory – General Fusion 2023 INFUSE Report

George K. Larsen (PI), Holly B. Flynn, and Paul A. Rowell

September 2023

SRNL-TR-2024-00326, Revision #1

Contents

List of Tables

List of Figures

List of Abbreviations

CECE	Combined Electrolysis Catalyst Exchange
CPP	Commercial Power Plant
DIR	Direct Internal Recycling
DT	Deuterium-Tritium
DOE FSS	Department of Energy Fusion Safety Standards
DT	Deuterium-Tritium
EP	Exhaust Processing
GD	Gas Detritiation
GLC	Gas Liquid Contactor
HX	Heat Exchanger
INFUSE	Innovation Network for Fusion Energy
IPTI	In-Process Tritium Inventory
IS	Isotope Separation
Li	Lithium
LLE	Lead Lithium Eutectic
$\dot{N}^-$	Tritium Burn Rate
NRC	Nuclear Regulatory Commission
OI	Operation Inventory
PAV	Permeation Against Vacuum
PCL	Power Conversion Loop
RHINO	Reduced Hydrogen Inventory Optimization
S&D	Storage and Delivery
SI	Startup Inventory
SRNL	Savannah River National Laboratory
TBR	Tritium Breeding Ratio
TBR_r	Required Minimum Tritium Breeding Ratio
TEP	Tritium Exhaust Processing
VST	Vacuum Sieve Tray
WD	Water Detritiation

Executive Summary

This report describes the results from an INFUSE research project, where Savannah River National Laboratory (SRNL) in collaboration with General Fusion (GF) used process modeling to understand and optimize commercial power plant (CPP) fuel cycle designs based on parameters provided by GF. The study primarily focused on two candidate fuel cycles with different blanket materials, one with a lead lithium eutectic (LLE) blanket and the other with a pure lithium (Li) blanket. LLE benefits from a low melting point, favorable neutronics, and lower reactivity, but liquid lithium has the potential for higher tritium breeding ratios (TBR) and does not poison the plasma as a high Z contaminant.

It was found that the main differences between LLE and Li designs are the extraction technologies required to remove tritium from the blanket and the amount of tritium and its distribution within the facility. More than 80% of the in-process tritium inventory for the LLE design is contained in the isotope separation system, while for the Li design, over 60% of the in-process tritium inventory is contained within the blanket material. This is due to significant tritium retention by Li. For the Li blanket, the burden of tritium processing rests on the blanket extraction technology rather than the traditional exhaust processing route. Thus, the blanket extraction technology is a main driver of tritium inventory in the Li system and determines the subsequent interface with the tritium processing plant.

Table 1 presents the startup inventories, plant doubling times, and TBRs for the both the GF LLE and Li blanket systems, as well as a comparison between Commonwealth Fusion System's ARC, ITER, and European DEMO parameters. Both GF designs have SI values comparable to ARC and significantly lower SI values as compared to both ITER and DEMO.

Table 1. Comparison of the need Startup Inventory, Plant Doubling Time, and TBR for the GF LLE and GF Li designs with values from ARC, ITER, and DEMO.

	Startup Inventory (kg)	Plant Doubling Time (days)	TBR
GF LLE	0.317	56	1.4
GF Li	0.747	67	1.8
ARC	0.3 – 1.5	730	1.08
ITER	~3.0	NA	NA
DEMO	4.0 – 10.0	1825	1.1-1.2

Introduction

Savannah River National Laboratory (SRNL) hosted General Fusion (GF) in-person on January 30th to 31st 2023 for the INFUSE kickoff meeting. During the two-day meeting, General Fusion presented detailed presentations about their design and design parameters. GF also supplied SRNL with a document that contained further design specifications[1]. In the GF device, Deuterium-Tritium (DT) fuel is injected into the chamber at 1 Hz. Initial design parameters included a lead lithium eutectic (LLE) as the blanket material, a burn fraction (β) of 0.0163*, fueling efficiency (η) of 25%*[1], tritium breeding ratio (TBR) of 1.40*, and a power output of ~500* MWth, resulting in a burn rate ($\dot{N}^{-}$) of 77.00 grams/day.

SRNL was then able to begin designing the system in both ASPEN and the reduced processing-time based RHINO (Reduced Hydrogen Inventory Optimization) model[2-4]. The document provided by GF allowed SRNL to back out tritium processing times for design specific subsystems, tritium extraction efficiencies, and LLE flow rates for the blanket. The document also detailed the breeder extraction technologies: gas-liquid contactor (GLC) and vacuum sieve tray (VST). SRNL would build designs for both extraction technologies and compare the results using different extraction efficiencies and processing times.

Part of Phase 1 involved bi-weekly meetings between SRNL and GF to discuss the parameters and ensure their system is being properly modelled. Initial discussions involved a lead lithium eutectic (LLE) for their blanket material; however, during these discussions GF determined that a pure lithium (Li) blanket is a better material for their design due to the negative effects of Pb in the fusion core. Thus, it was requested to understand the fuel cycle implications of a change from LLE to Li. The tritium extraction technology that was selected to be explored with a pure Li blanket is: SRNL's LiT electrolysis method[5] and the Maroni process[6].

This report is broken down into three main sections. The first section will be the overview and results of the LLE blanket design. This section will also describe how the data was analyzed and introduce key equations and technology selection. Next, the results and information from and about the Li blanket design will be introduced. A discussion section will report on differences between the designs, key parameters and uncertainties from each design as they compare to past, present, and future designs, DOE Fusion Safety Standards (FSS), and Nuclear Regulatory Commission (NRC) site regulations. The final section will conclude the report. Following the report is a bibliography of references and three appendices. Appendix 1 describes the process parameters used for both the LLE and Li designs for each subsystem. The parameters contained in this appendix are the values used for all calculations except when otherwise stated. Appendix 2 contains data plots and information calculated during this project that are auxiliary to the primary objective, and Appendix 3 details out specific technology (e.g Pd diffuser bank) and how the processing times were calculated using described specifications.

[1] *These values were provided by General Fusion

LLE Blanket Design and Technology Selection

Figure 1 shows the ASPEN block diagram for the GF fuel cycle design with the LLE blanket. Table 9 in Appendix 1 is an accompanying image describing the technology represented by each block according to its flow stream.

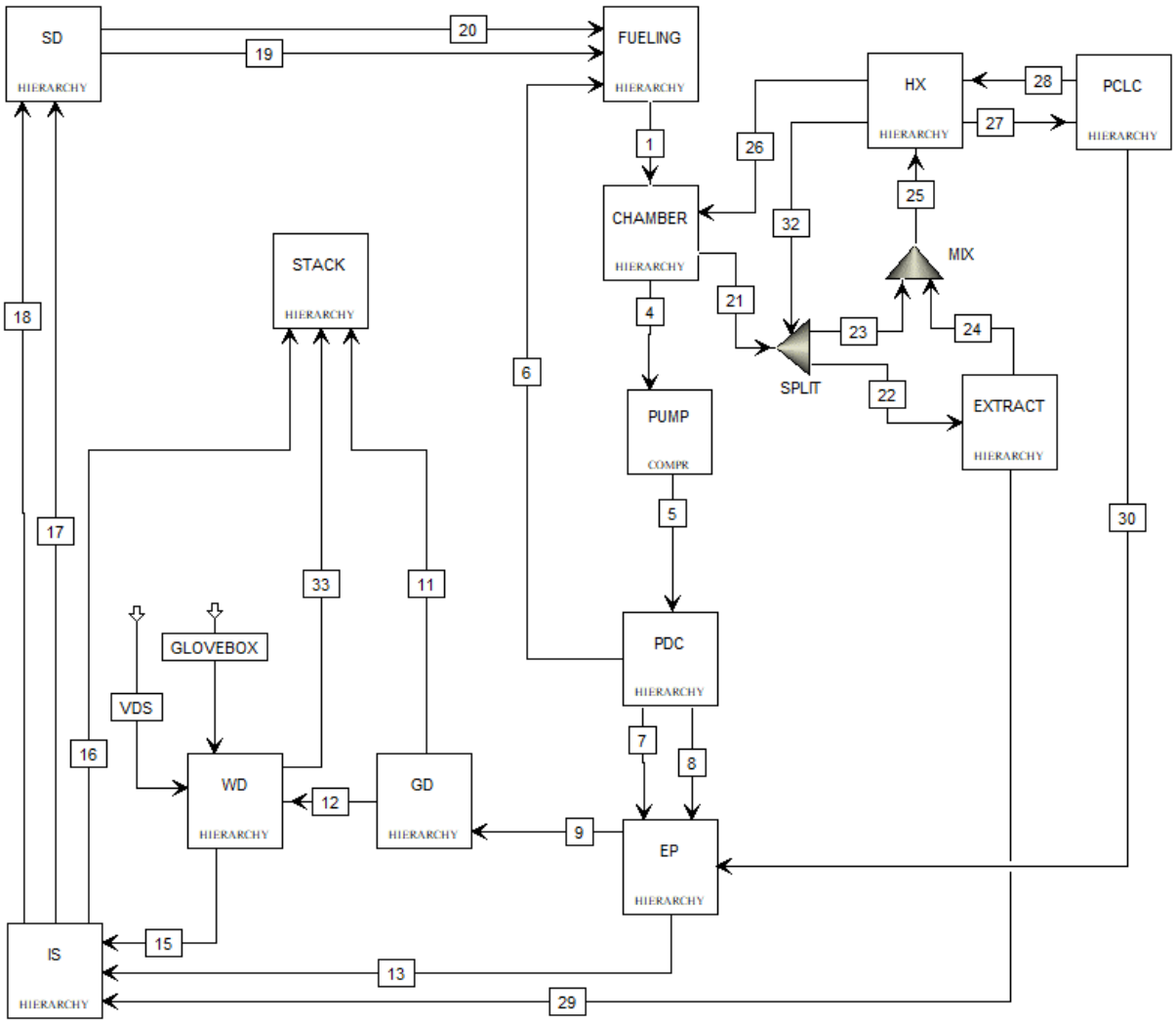

Figure 1. The block diagram used to describe the GF device for the RHINO code.

Table 2: Modeled system blocks and their represented technologies in Aspen Plus and RHINO as outlined in Figure 1.a

System Block	Technology
Pump	Continuous Pumping
Palladium Cleanup (PDC)	Palladium Diffusers
Exhaust Processing (EP)	Palladium Diffusers
Gas Detritiation (GD)	Molecular Sieve Beds**
Water Detritiation (WD)	Combined Electrolysis Catalyst Exchange (CECE) **
Isotope Separation (IS)	Cryogenic Distillation**
Fueling	Gas Puffing*
Heat Exchanger (HX)*	Counter-Current Heat Exchanger**
Power Conversion Loop Cleanup (PCLC)	Palladium Diffusers
Extract – LLE Blanket	Gas Liquid Contactor/VST**
Extract – Lithium Blanket	Electrolysis/Maroni

*Values provided by General Fusion; **Values provided by reference 1; ***Values calculated using Appendix 3

The technologies selected for the fuel cycle model were informed by reference [1], provided by General Fusion personnel, or decided upon by the highest acceptable TRL. CNL's analysis of the GF fusion pilot plant outlines suggested technologies for many systems that were selected in Table 2 above. Pumping was simplified in the model to serve the purpose of altering the pressure of a continuously flowing stream without representing any specialized technology. Palladium diffusers are selected as the technology for first stage hydrogen separation and are utilized in a direct internal recycling (DIR) configuration to minimize tritium inventory. Molecular sieve beds are widely used and available to serve the function of a precursor to water detritiation (WD) in the gas detritiation (GD) unit to allow for the removal of stackable gases. Water detritiation is assumed to be performed onsite so combined electrolysis catalytic exchange (CECE) is selected as the technology based on the precedence of use at ITER. Isotope separation was modeled as cryogenic distillation columns due to its high TRL and highly scalable throughput.

A counter current heat exchanger was selected due to the straightforward comparison between multiple materials. In the power conversion loop, a cleanup system would be required to remove the hydrogen isotopes that permeate through the heat exchanger. It is assumed that the heat exchanger does not directly interface the blanket with water due to the difficulty and cost of water detritiation. In addition, the current model assumes a continuous extraction system, such as Pd diffuser, to simplify the computation. However, in a helium-based system, hydrogen getters would likely be the optimal solution. The batch mode operation of these getters would increase the inventory within that loop, but since the inventory in that system is very small, it would have negligible effect on the overall plant balance.

The blanket extraction system depends on the selection of either LLE or Li and both were modeled using their respective properties such as extraction efficiency and processing time across the two blanket materials and their compatibility with available technology choices. This led to the

consideration of multiple options for both LLE and lithium to better understand the performance. More on technology sizing, calculations, and assumptions can be found in Appendix 3.

Baseline simulations were performed for this LLE design using parameters described in the Appendix 1. This section reports on the calculated startup inventory (SI) described in Equation 1.

$$SI = I_{req} + 20\%\ contingency \qquad Equation\ 1$$

The 20% contingency is a value selected by SRNL based on historical efforts but is left up to the discretion of General Fusion. However, if the contingency is 0% then the Storage and Delivery system will reach a zero-tritium inventory resulting in insufficient tritium to supply and operate the plant. The 20% contingency is also put in place to offset losses due to material uptake in the system during startup. Figure 2 is a mock plot of the time-dependent inventory in Storage and Delivery over time. SI is represented by the magenta dashed segment and is shown to be the sum of I_{req} and the 20% contingency as described in Equation 1. I_{req} is the difference between the initial inventory (I_0) and the minimum inventory (I_{min}) in S&D. This value is dominated by the In-Process Tritium Inventory (IPTI) needs and can be described in more detail by Equation 2.

$$I_{req} = I_0 - I_{min} = \int_{t=0}^{t=t_{min}} (process - loss)dt \qquad Equation\ 2$$

In Equation 2 *process* is the added flow of tritium that makes it to S&D from breeding and fueling and *loss* is the tritium lost through radioactive decay, stacked loss, and that gets held up in the processing systems until steady state operation is met. Once the system has reach steady state operation all processing components have reached a near steady state inventory. This occurs when S&D has reached a minimum inventory (I_{min}), which is shown by the inflection point in Figure 2. Once this point has been reached the amount bred just has to overcome the losses from radioactive decay and the stack, hence the increase in S&D inventory.

Once the inventory in S&D has reached an amount equal to the sum of SI and the Operation Inventory (OI), tritium can be moved offsite for sell or to startup a new plant. This is called the plant doubling time (t_d) and is represented in Figure 2 by the blue dashed segment. OI is described in Equation 3.

$$OI = \left(\frac{\dot{N}^-}{\beta\eta}\right) t_r\left(1 - DR_{frac}\right) \qquad Equation\ 3$$

In the above equation, t_r is the amount of time allotted to operate on a tritium reserve inventory. This reserve inventory is a function of the plant's maintenance plans and preferences. For the purpose of this study, t_r has been set to 24 hrs. General Fusion can be more or less conservative with this value based on plant design, cost, and requirements. For example, the more redundancies implemented the shorter t_r can be, but this would increase the plant overall cost. The combination of the reserve inventory and DR_{frac}, the fraction of inventory flow that is returned to fueling by Direct Internal Recycling (DIR), enables a plant to continue operation and power production if a downstream system or series of systems undergoes unplanned maintenance or issues. For this study and based on the General Fusion design DIR_{frac} has been set to 0.95[7].

Figure 3 shows the time-dependent inventory in storage and delivery (S&D). In the figure, the calculated SI and I_{req} are represented by magenta (317 grams) and gray (264 grams) dashed line-

segments, respectively. The plant doubling time (t_d) occurs at 41 days. I_{req} is dominated by the amount needed to fill all processing components during startup, which is driven by a subsystem's or series of subsystem's processing time and inlet flow fraction. If the processing time is increased either due to new technology, changes in flow or footprint, or redundancies then I_{req} will increase. For this system the total IPTI is 303 grams.

Figure 4 shows the IPTI for the different processing components of the LLE blanket fuel cycle design. It is important to note that the isotope separation system (IS) makes up > 80% of the IPTI, which is a result of its high processing time. In this system, IS is a cryogenic distillation column. The annual amount of tritium lost out the stack for the GF LLE design is ~0.012 grams. This calculation was done at optimal operations and did not account for any maintenance scenarios such as an open glovebox maintenance, which would increase the tritium emissions from the plant.

Figure 5 shows the steady state inventory of the blanket extraction system for the LLE blanket design across varied extraction efficiencies and increasing processing times. The boxed values represent expected operating conditions for technologies of interest, which are GLC (gas liquid contactors) in black, VST (vacuum sieve tray) and PAV (permeation against vacuum) in blue. The results show that the steady state inventory of the blanket is not a concern unless the selected technology has very poor operating conditions and are outside of expected bounds.

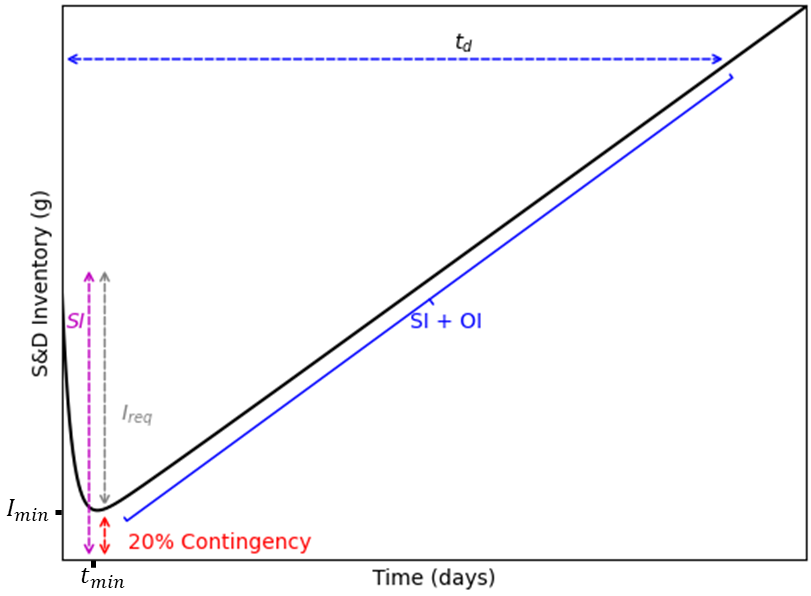

Figure 2. A mock plot demonstrating key values for the operation of a fusion fuel cycle, including Startup Inventory (SI) (magenta), I_{req} (grey), the 20% contingency (red), and t_d (blue). SI is shown to be equal to the sum of I_{req} and the 20% contingency and t_d is shown to be the point at which the inventory in Storage and Delivery equals the Starting Inventory plus the Operational Inventory. I_{min} is the point at which the system has reached near steady state conditions and all processing components have a max processing inventory.

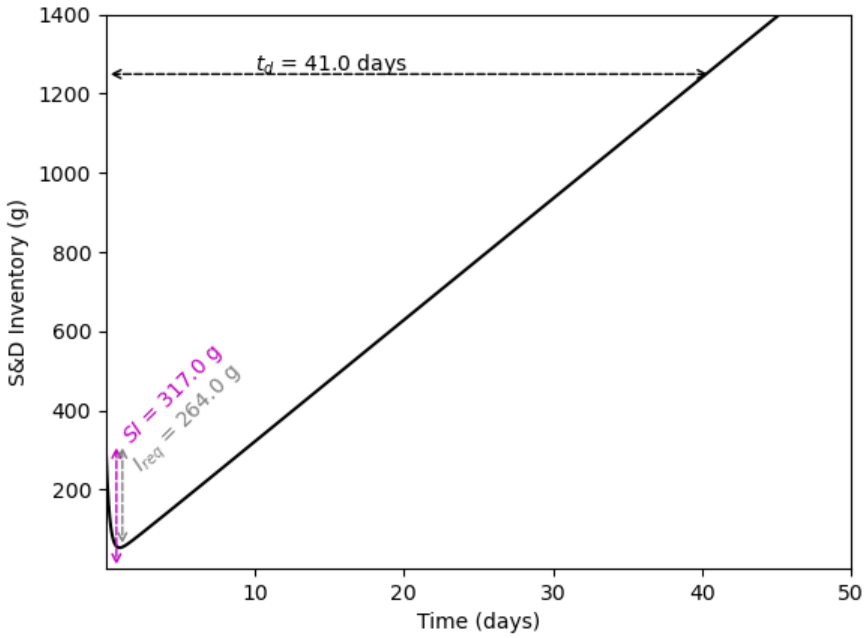

Figure 3. Storage and Delivery time-dependent inventory showing the values for SI, t_d, T_{min}, and I_{req}.

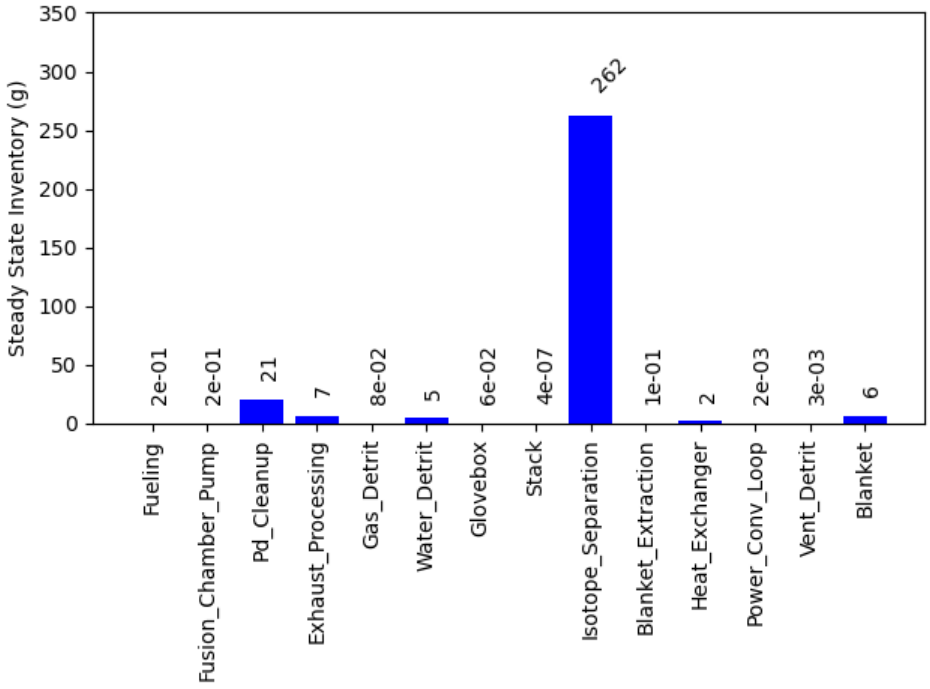

Figure 4. Steady-state inventory of each individual subsystem in the GF LLE design.

		1 second	10 seconds	30 seconds	1 minute	5 minutes	10 minutes	30 minutes	1 hour	2 hours	5 hours
		Processing Time (seconds)									
		1	10	30	60	300	600	1800	3600	7200	18000
Extraction Efficiency	5%	2.4E-02	2.4E-01	7.3E-01	1.5E+00	7.3E+00	1.5E+01	4.4E+01	8.8E+01	1.8E+02	4.4E+02
	10%	1.2E-02	1.2E-01	3.7E-01	7.4E-01	3.7E+00	7.4E+00	2.2E+01	4.4E+01	8.8E+01	2.2E+02
	15%	8.2E-03	8.2E-02	2.5E-01	4.9E-01	2.5E+00	4.9E+00	1.5E+01	3.0E+01	5.9E+01	1.5E+02
	20%	6.2E-03	6.2E-02	1.9E-01	3.7E-01	1.9E+00	3.7E+00	1.1E+01	2.2E+01	4.4E+01	1.1E+02
	25%	4.9E-03	4.9E-02	1.5E-01	3.0E-01	1.5E+00	3.0E+00	8.9E+00	1.8E+01	3.6E+01	8.9E+01
	30%	4.1E-03	4.1E-02	1.2E-01	2.5E-01	1.2E+00	2.5E+00	7.4E+00	1.5E+01	3.0E+01	7.4E+01
	35%	3.5E-03	3.5E-02	1.1E-01	2.1E-01	1.1E+00	2.1E+00	6.4E+00	1.3E+01	2.5E+01	6.4E+01
	40%	3.1E-03	3.1E-02	9.3E-02	1.9E-01	9.3E-01	1.9E+00	5.6E+00	1.1E+01	2.2E+01	5.6E+01
	45%	2.8E-03	2.8E-02	8.3E-02	1.7E-01	8.3E-01	1.7E+00	5.0E+00	9.9E+00	2.0E+01	5.0E+01
	50%	2.5E-03	2.5E-02	7.4E-02	1.5E-01	7.4E-01	1.5E+00	4.5E+00	8.9E+00	1.8E+01	4.5E+01
	55%	2.3E-03	2.3E-02	6.8E-02	1.4E-01	6.8E-01	1.4E+00	4.1E+00	8.1E+00	1.6E+01	4.1E+01
	60%	2.1E-03	2.1E-02	6.2E-02	1.2E-01	6.2E-01	1.2E+00	3.7E+00	7.4E+00	1.5E+01	3.7E+01
	65%	1.9E-03	1.9E-02	5.7E-02	1.1E-01	5.7E-01	1.1E+00	3.4E+00	6.9E+00	1.4E+01	3.4E+01
	70%	1.8E-03	1.8E-02	5.3E-02	1.1E-01	5.3E-01	1.1E+00	3.2E+00	6.4E+00	1.3E+01	3.2E+01
	75%	1.7E-03	1.7E-02	5.0E-02	9.9E-02	5.0E-01	9.9E-01	3.0E+00	5.9E+00	1.2E+01	3.0E+01
	80%	1.5E-03	1.5E-02	4.6E-02	9.3E-02	4.6E-01	9.3E-01	2.8E+00	5.6E+00	1.1E+01	2.8E+01
	85%	1.5E-03	1.5E-02	4.4E-02	8.7E-02	4.4E-01	8.7E-01	2.6E+00	5.2E+00	1.0E+01	2.6E+01
	90%	1.4E-03	1.4E-02	4.1E-02	8.3E-02	4.1E-01	8.3E-01	2.5E+00	5.0E+00	9.9E+00	2.5E+01
	95%	1.3E-03	1.3E-02	3.9E-02	7.8E-02	3.9E-01	7.8E-01	2.3E+00	4.7E+00	9.4E+00	2.3E+01
	100%	1.2E-03	1.2E-02	3.7E-02	7.4E-02	3.7E-01	7.4E-01	2.2E+00	4.5E+00	8.9E+00	2.2E+01
		Steady State Inventory of Extraction System - PbLi Blanklet (grams)									

Figure 5. Steady-state inventory heat map of the extraction system across varied efficiencies and processing times for LLE assuming 90% of the blanket flow bypasses the extraction system. Black box representing GLC and Blue box representing VST/PAV.

Li Blanket Design

Figure 6 shows the ASPEN block diagram for the GF fuel cycle design with the Li blanket. Table 10 in Appendix 1 is an accompanying image describing the technology represented by each block according to its flow stream.

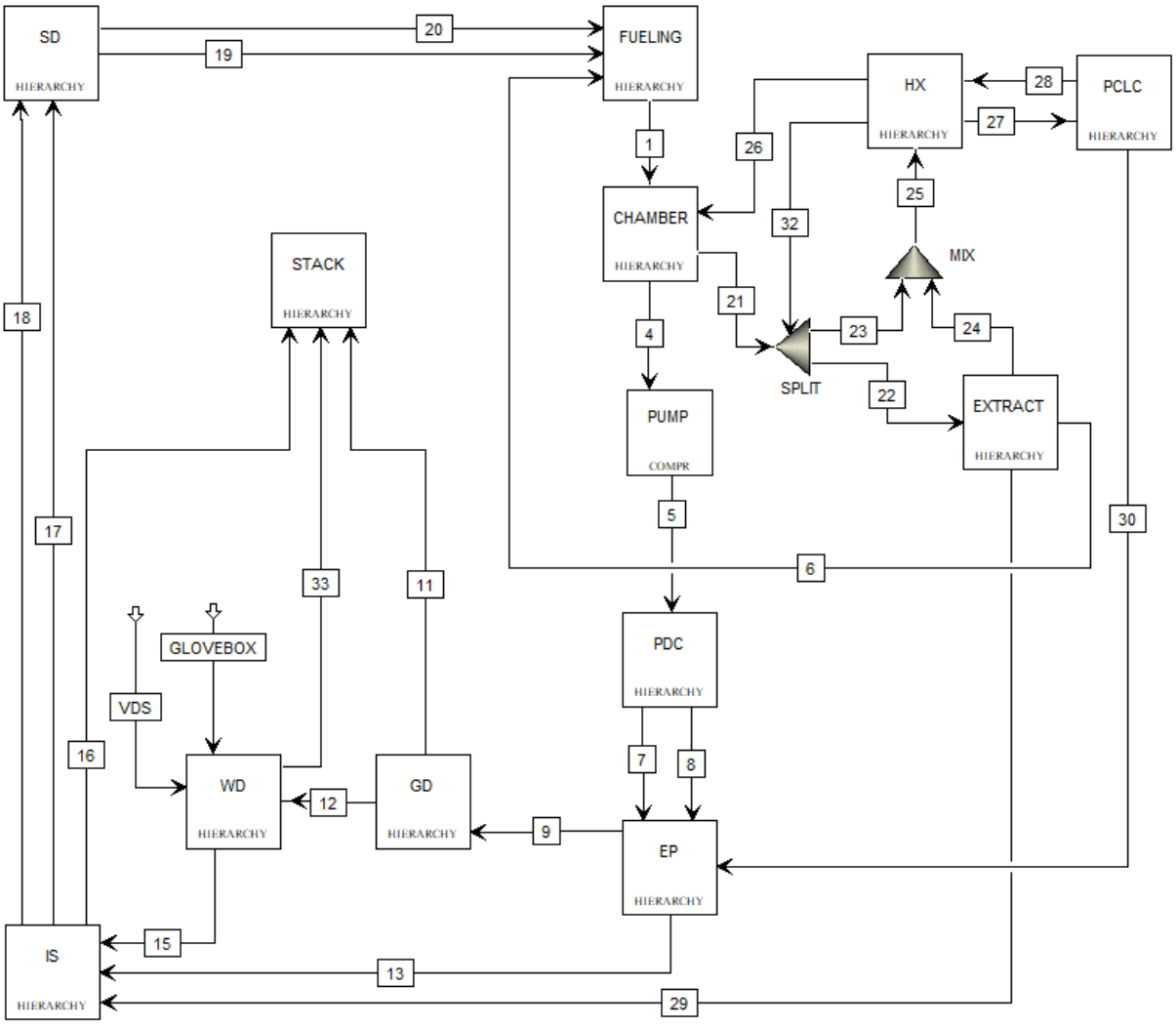

Figure 6. The block diagram used to describe the GF Li device for the RHINO and ASPEN code.

The Li blanket design varies from the LLE blanket design due to the very high retention of tritium fuel by the lithium (>99%) due to contact in the fusion chamber. The neutral flow of hydrogen ($155\,\frac{mols}{hr}$) will be completely retained in the lithium blanket since it is $\ll$ 0.1-0.2% of the $5.2 \times 10^8\,\frac{mols}{hr}$ lithium flow rate,[8] and the hydrogen ions in the plasma will be completely retained in the flowing lithium[9]. The uptake of the DT fuel into the blanket moves the burden of processing from the chamber exhaust to the blanket extraction system. In Figure 6 the entrance to the DIR stream (6) has been moved from the palladium cleanup (PdC) to the blanket extraction (EXTRACT) system. 95% of the removed hydrogen isotopes exiting EXTRACT go to Fueling.

Figure 7 shows the time-dependent inventory in S&D. In the figure, the calculated SI and I_{req} are represented by magenta (793 grams) and gray (661 grams) dashed line-segments, respectively. The annual stacked tritium is 0.035 grams and the total IPTI is 747 grams. Figure 8 shows the IPTI for the different processing components of the Li blanket fuel cycle design. Unlike LLE the majority of tritium inventory (> 60%) is held up in the lithium Blanket material, whereas 35% is in IS. This means that the processing burden has been shifted to the outlet of the blanket extraction system and more emphasis needs to be placed on the extraction system. The better the extraction efficiency and allowable flow rate into the extraction technology the lower the SI and the IPTI in the blanket. For the calculation of the SI and IPTI the extraction efficiency was set to 20% due to the low TRL of the lithium extraction technology, but Figure 9 shows the steady state inventory of the blanket extraction system across varied extraction efficiencies and increasing processing times. The two technology choices looked at for tritium extraction out of the lithium blanket were the Maroni Process (blue box) and LiT Electrolysis (black box).

For the Maroni process the suggested configuration of a parallel network of centrifugal contactors, 25 cm diameter and 45 cm height, was used resulting in a need for 314 units to handle the full throughput of 2 m^3/s of Li[6]. Each unit has a processing time on the order of 2.7 seconds and draws 3.7 kW of power during continuous operation with an extraction efficiency of 20%. The full setup of 314 units would then draw <1.2 MW for the operation of the centrifugal contactors and an expected power consumption of <1 kW for the electrolysis tritium evolution. By varying the slipstream that splits the blanket flow between the heat exchanger and extraction system the number of units and power consumption will both decrease to match the throughput.

LiT Electrolysis functions very closely to a continuously stirred tank reactor with the reaction rate and residence time being the main considerations. The residence time of your unit is tied to the flowrate and volume of the system, while the extraction efficiency is proportional to the surface area of the electrode. The LiT electrolysis process itself has little concern for power draw as running the electrode consumes power on the order of kilowatts, but the process is in its infancy and will require more research to determine to what level of throughput it can handle. With the current TRL being low it is difficult to accurately determine hard values for these parameters but in theory they could be tuned to fit in the desired fuel cycle conditions for a given system design.

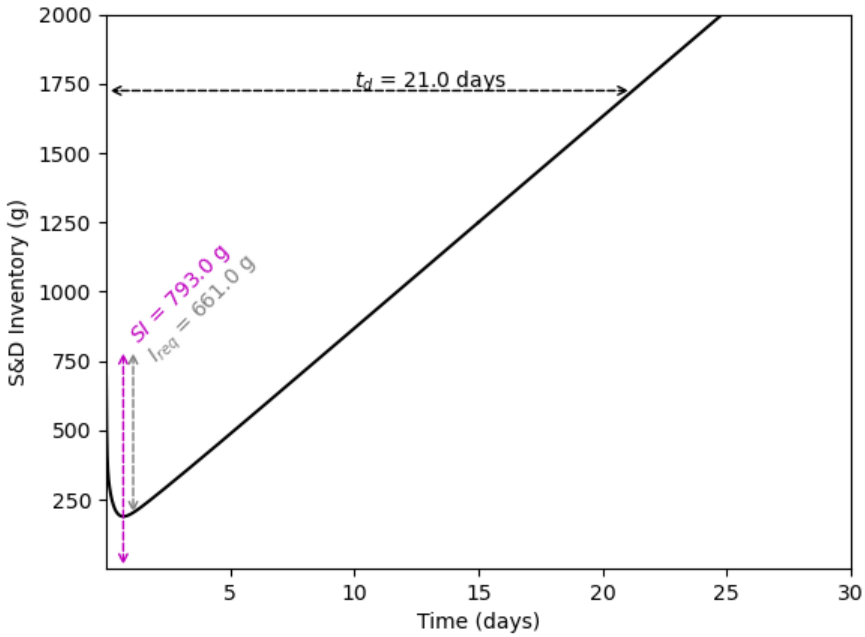

Figure 7. Storage and Delivery time-dependent inventory showing the values for SI, t_d, T_{min}, and I_{req}.

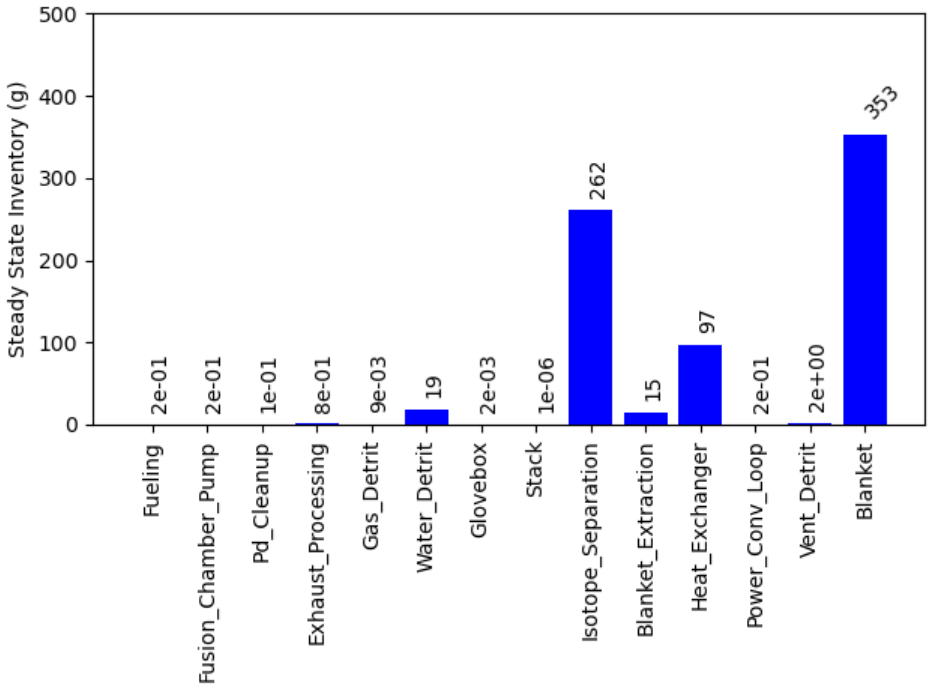

Figure 8. Steady-state inventory of each individual subsystem in the GF LLE design.

Extraction Efficiency	1 second	10 seconds	30 seconds	1 minute	5 minutes	10 minutes	30 minutes	1 hour	2 hours	5 hours
	Processing Time (seconds)									
	1	10	30	60	300	600	1800	3600	7200	18000
5%	4.1E+00	4.1E+01	1.2E+02	2.4E+02	1.2E+03	2.4E+03	7.3E+03	1.5E+04	2.9E+04	7.3E+04
10%	1.9E+00	1.9E+01	5.8E+01	1.2E+02	5.8E+02	1.2E+03	3.5E+03	7.0E+03	1.4E+04	3.5E+04
15%	1.2E+00	1.2E+01	3.7E+01	7.4E+01	3.7E+02	7.4E+02	2.2E+03	4.4E+03	8.8E+03	2.2E+04
20%	8.7E-01	8.7E+00	2.6E+01	5.2E+01	2.6E+02	5.2E+02	1.6E+03	3.1E+03	6.3E+03	1.6E+04
25%	6.6E-01	6.6E+00	2.0E+01	3.9E+01	2.0E+02	3.9E+02	1.2E+03	2.4E+03	4.7E+03	1.2E+04
30%	5.1E-01	5.1E+00	1.5E+01	3.1E+01	1.5E+02	3.1E+02	9.2E+02	1.8E+03	3.7E+03	9.2E+03
35%	4.1E-01	4.1E+00	1.2E+01	2.5E+01	1.2E+02	2.5E+02	7.4E+02	1.5E+03	3.0E+03	7.4E+03
40%	3.3E-01	3.3E+00	1.0E+01	2.0E+01	1.0E+02	2.0E+02	6.0E+02	1.2E+03	2.4E+03	6.0E+03
45%	2.8E-01	2.8E+00	8.3E+00	1.7E+01	8.3E+01	1.7E+02	5.0E+02	9.9E+02	2.0E+03	5.0E+03
50%	2.3E-01	2.3E+00	6.8E+00	1.4E+01	6.8E+01	1.4E+02	4.1E+02	8.2E+02	1.6E+03	4.1E+03
55%	1.9E-01	1.9E+00	5.6E+00	1.1E+01	5.6E+01	1.1E+02	3.4E+02	6.8E+02	1.4E+03	3.4E+03
60%	1.6E-01	1.6E+00	4.7E+00	9.3E+00	4.7E+01	9.3E+01	2.8E+02	5.6E+02	1.1E+03	2.8E+03
65%	1.3E-01	1.3E+00	3.8E+00	7.7E+00	3.8E+01	7.7E+01	2.3E+02	4.6E+02	9.2E+02	2.3E+03
70%	1.0E-01	1.0E+00	3.1E+00	6.3E+00	3.1E+01	6.3E+01	1.9E+02	3.8E+02	7.5E+02	1.9E+03
75%	8.4E-02	8.4E-01	2.5E+00	5.1E+00	2.5E+01	5.1E+01	1.5E+02	3.0E+02	6.1E+02	1.5E+03
80%	6.6E-02	6.6E-01	2.0E+00	4.0E+00	2.0E+01	4.0E+01	1.2E+02	2.4E+02	4.8E+02	1.2E+03
85%	5.1E-02	5.1E-01	1.5E+00	3.0E+00	1.5E+01	3.0E+01	9.1E+01	1.8E+02	3.6E+02	9.1E+02
90%	3.6E-02	3.6E-01	1.1E+00	2.2E+00	1.1E+01	2.2E+01	6.6E+01	1.3E+02	2.6E+02	6.6E+02
95%	2.4E-02	2.4E-01	7.2E-01	1.4E+00	7.2E+00	1.4E+01	4.3E+01	8.6E+01	1.7E+02	4.3E+02
100%	1.3E-02	1.3E-01	3.8E-01	7.6E-01	3.8E+00	7.6E+00	2.3E+01	4.5E+01	9.1E+01	2.3E+02
	Steady State Inventory of Extraction System - Li Blanket (grams)									

Figure 9. Steady-state inventory heat map of the extraction system across varied efficiencies and processing times for Li assuming 50% of the blanket flow bypasses the extraction system. Black box representing LiT Electrolysis and Blue box representing Maroni.

Discussion

The most significant difference between the two blanket designs is the required physical design of the power plant. For the LLE blanket design, the system is very similar to other contemporary designs. This system utilizes higher TRL processing subsystems and the highest amount of IPTI (>80%) is held up in the isotope separation system. For the Li blanket design, the lithium blanket material acts as a getter for the hydrogen and its isotopes. This means that a large portion of the total IPTI (>60%) is held up in the liquid lithium circulating through the blanket systems and the fusion chamber. Due to the increase in IPTI in the blanket systems the fractional flow split between the blanket extraction system and the heat exchanger needs to be high. This means that a larger portion of the flow needs to move through the blanket extraction technology and the extraction technology needs a >20% extraction efficiency. The plots in the previous section were calculated with 90% of the blanket material flowing through the blanket extraction system with a 20% extraction efficiency.

Furthermore, the increase in blanket inventory requires that the main tritium processing be done after the blanket extraction system. This moves the processing load from the exhaust of the fusion chamber to the outlet of the blanket. So, the design for the Li blanket option needs to have DIR implemented directly after the blanket extraction system and there needs to be some mitigation system that controls the flow of isotopes to the isotope separation system. The flow rate entering the Pd cleanup stage in the exhaust stream is orders of magnitude lower (0.0045 $\frac{m^3}{min}$) than the LLE blanket design (0.1797 $\frac{m^3}{min}$). This value impacts the size of the Pd Cleanup phase (reference Appendix 3) and its processing time.

Table 3. Comparison of the need Startup Inventory, Plant Doubling Time, and TBR for the GF LLE and GF Li designs with values from ARC, ITER, and DEMO.

	Startup Inventory (kg)	Plant Doubling Time (days)	TBR
GF LLE	0.317	56	1.4
GF Li	0.747	67	1.8
ARC	0.3* – 1.5	730	1.08
ITER	~1.2 - 18.5**	NA	NA
DEMO	4.0 – 10.0	1825	1.1-1.2

*Required significant improvements in fuel cycle technologies and plasma operations and calculated using Abdou's equation.[10]
**ITER will not have production of tritium so expected over the lifetime to consume ~18 kg[11, 12]

For illustrative purposes, Table 3 presents the startup inventory, plant doubling time, and TBR of both LLE and Li designs and compares them with other fuel cycle parameters: ITER, the European Union's DEMO, and Commonwealth Fusion System's ARC. Table 5 shows the tritium effluent released per year for the operation of the GF LLE and GF Li design as compared to the maximum exposure to the public during normal operations for the Nuclear Regulatory Commission (NRC) (1 mSv/yr)[13] and the Department of Energy Fusion Safety Standards (DOE FSS) (0.1

mSv/yr)[14]. Both facilities are well below the General Site Regulation Limits and more than 8 times less than the General Site Goals per year.

Table 4. The tritium amount in grams per year released from the stack for the GF LLE and GF Li as compared to site regulation limits.

	Tritium Stacked (g/year)
GF LLE	0.012
GF Li	0.035
NRC (g/yr)	2.860
DOE FSS (g/yr)	0.286

Conclusion

The modeling effort was performed using data and assumptions available on the current state of technology. Both the GF LLE and GF Li designs are feasible systems with inventories and release values within or below limits. However, results from the study highlighted that for the GF Li design the blanket technology is going to be the most critical and key technologies to success. The calculated inventory in the blanket material will be greater than 300 grams; therefore, it is recommended that Research and Development (R&D) efforts should be focused on optimizing the blanket technology. This includes optimizing the blanket extraction system so that greater than 50% is removed from the blanket and reducing the processing times to reduce inventory hold up. The blanket inventory will also include protium and deuterium and understanding the impact this increased inventory has on the system will be important. It is also significant to report that all inventory numbers above would improve if the fueling efficiency was increased from 25%.

Appendix 1: General Fusion Design Parameters

Table 5 lists the processing times (T_i) of each subsystem for both the LLE and Li designs. Processing times are quantitative representations of the amount of time it takes for tritium to move through the system. The RHINO model is a reduced model that calculates the time dependent inventories based on the implementation of processing times for each subsystem in the fuel cycle.

Table 5. Processing times (T_i) of each subsystem in the GF LLE and Li designs.

Index, i	Name	LLE Processing Times, T_i (min)	Li Processing Times, T_i (min)
0	Storage Delivery	0.0000	0.0000
1	Fueling	0.0167*	0.0167*
2	Fusion Chamber and Pump	0.0154*	0.0154*
3	Pd Cleanup	1.5840***	1.5840***
4[5]	Exhaust Processing	10.1952	10.1952
5[15-17]	Gas Detritiation	119.9520	119.9520
6[5]	Water Detritiation	2880.000	2880.000
7[7]	Glovebox	60.0480	60.0480
8[5]	Stack	16.7040	16.7040
9[6]	Isotope Separation	360.000	360.000
10[5]	Extraction Technology	0.9994	TBD
11	Heat Exchanger	1.5840**	0.8338*
12[6]	Power Conversion Loop	16.704	16.704
13	Vent Detritiation	240.480	240.480
14[5]	Blanket		

*Values provided by General Fusion; **Values provided by reference 1; ***Values calculated using Appendix 3

Table 6 lists each subsystem's process name, index (i), fractional loss not due to radioactive decay (ϵ_i), and the feed subsystem's index (j) and fractional flow ($F_{j\to i}$) into i. The fractional loss not due to radioactive decay for each subsystem is dominated by permeation. The inventory lost due to permeation is lost only from the specific subsystem and not the total system. Inventory that permeates out of a subsystem is captured by a secondary confinement system, such as a glovebox, and re-introduced to the system either in the water detritiation system or the gas detritiation system. Subsystems that undergo high temperatures have ϵ_i values greater than 0 and these values are pulled from the literature references provided.

Table 6. List of each subsystem with its non-radioactive loss term (ε_i), index of subsystem(s) that flow into subsystem *I* (j), and each fractional flow of those subsystems into subsystem *i* ($F_{j\to i}$.

Index, i	**Name**	**Non-Radioactive Losses, ε_i**	**Index of Contributing Subsystems, j**	**Fractional Flow, $F_{j\to i}$**
0	Storage Delivery	0.00000	[3,9]	[0.95000,1.00000]
1	Fueling	0.00000	None	[0.00000]
2	Fusion Chamber and Pump	0.00000	[1]	[1.00000]
3	Pd Cleanup	0.00005	[2]	[1.00000]
4[5]	Exhaust Processing	0.00050	[3,12]	[0.05000,1.000]
5[15-17]	Gas Detritiation	0.00000	[4]	[0.50000]
6[5]	Water Detritiation	0.00000	[5,7,13]	[0.99999,1.000,1.000]
7[7]	Glovebox	0.00000	Losses from 3,4, and 6	None
8[5]	Stack	0.00000	[5,6]	[0.00001,0.00001]
9[6]	Isotope Separation	0.00000	[4,6,10]	[0.500,0.99999,0.600]
10[5]	Extraction Technology	0.00000	[14]	[0.10000]**
11	Heat Exchanger	0.00010	[10,14	[0.40000,0.90000**]
12[6]	Power Conversion Loop	0.00010	Losses from 11	[0.00000]
13	Vent Detritiation	0.00000	Losses from 2,9,10,12	[0.10000]
14[5]	Blanket	0.00000	[11]	[1.00000*]

*Values provided by General Fusion; **Values provided by reference 1; ***Values calculated using Appendix 3

Table 7 lists the burn fraction (β), fueling efficiency (η), burn rate ($\dot{N}^-$), tritium breeding ratio (TBR), and source terms for different subsystems (S_i). The source terms are constant flow rate values supplied to a subsystem that is not connect to a processing time. Storage and Delivery (S&D) provides 18,895.71 $\frac{grams}{day}$ to fueling. This is a constant calculated based β, η, and $\dot{N}^-$ and represents the amount of available fuel required in fueling to maintain the targeted output. The blanket receives a value equal to the product of the TBR and $\dot{N}^-$, which represents the amount of tritium bred and added to the system. The burn rate, $\dot{N}^-$, is calculated based on the thermal power output of each system (see Appendix 3).

Table 7. List of fuel cycle parameters for both the LLE and Li blanket designs.

Parameter	LLE Blanket	Li Blanket	Units
β	0.0163*	0.0206*	
η	0.25*	0.25*	
$\dot{N}^-$	77*,***	96*,***	grams/day
TBR	1.40*	1.25/1.80*	
S&D S_i	-18,895.71	-18,640.78	grams/day
Fueling S_i	18,895.71	18,640.78	grams/day
Blanket S_i	$\dot{N}^- xTBR$	$\dot{N}^- xTBR$	grams/day

*Values provided by General Fusion; **Values provided by reference 1; ***Values calculated using Appendix 3

Table 8 and Table 9 is a list of all the subsystem flows from Figure 1 and Figure 6, respectively. The first column lists the stream number indicated in the figures. The stream number is found on each figure at the center of lines connecting two separate subsystem blocks. The Origin and Destination columns list the the subsystems that the flow begins at (Origin) and ends at (Destination). The Destination subsystem is also indicated by the arrow of the line segment containing the stream number.

Table 8. The flow channel stream number from Figure 1's ASPEN block diagram with origin and destination blocks indicated.

Stream	Origin	Destination
1	Fueling	Chamber
4	Chamber	Exhaust
5	Exhaust	PDC
6	Palladium Cleanup	Fueling
7		Exhaust Processing
8		
9	Exhaust Processing	Gas Detritiation
11	Gas Detritiation	Stack
12		Water Detritiation
13	Exhaust Processing	Isotope Separation
15	Water Detritiation	
16	Isotope Separation	Storage & Delivery
17		
18		
19	Storage & Delivery	Fueling
20		
21	Chamber	Slipstream
22	Slipstream	Blanket Extraction
23	Slipstream	Heat Exchanger
24	Blanket Extraction	
25	Mixed Slipstream	
26	Heat Exchanger	Chamber
27		Power Conversion Loop
28	Power Conversion Loop	Heat Exchanger
29	Blanket Extraction	Isotope Separation
30	Power Conversion Loop	Exhaust Processing
32*	Heat Exchanger	Slipstream
33	Water Detritiation	Stack
VDS	Vent Detritiation	Water Detritiation
GB	Glovebox	

Table 9. The flow channel stream number from Figure 6's ASPEN block diagram with origin and destination blocks indicated.

Stream	Origin	Destination
1	Fueling	Chamber
4	Chamber	Exhaust
5	Exhaust	PDC
6	Blanket Extraction	Fueling
7	Palladium Cleanup	Exhaust Processing
8		
9	Exhaust Processing	Gas Detritiation
11	Gas Detritiation	Stack
12		Water Detritiation
13	Exhaust Processing	Isotope Separation
15	Water Detritiation	
16	Isotope Separation	Storage & Delivery
17		
18		
19	Storage & Delivery	Fueling
20		
21	Chamber	Slipstream
22	Slipstream	Blanket Extraction
23	Slipstream	Heat Exchanger
24	Blanket Extraction	
25	Mixed Slipstream	
26	Heat Exchanger	Chamber
27		Power Conversion Loop
28	Power Conversion Loop	Heat Exchanger
29	Blanket Extraction	Isotope Separation
30	Power Conversion Loop	Exhaust Processing
32*	Heat Exchanger	Slipstream
33	Water Detritiation	Stack
VDS	Vent Detritiation	Water Detritiation
GB	Glovebox	

Appendix 2: Data Plots

A. LLE Design Data Plots

Figure 10 shows the time dependent inventory for all subsystems in the LLE design and the point at which they reach a steady state inventory. The higher the processing time the longer it takes for subsystem to reach steady state inventories and hence the higher the in-process inventory in that subsystem. Improvements in processing time directly impact the amount of inventory held up in the system. Another factor that impacts subsystem in-process inventory is the fractional flow into the subsystem. For example, water detritiation has the highest processing time of 2 days, but the isotope separation system has a significantly higher in-process tritium inventory (Figure 4). This is because the flow from gas detritiation is limited and kept low to avoid a buildup in the system[18]. This is possible by using ambient molecular sieve beds (AMSB) and palladium membrane reactors (PMR).

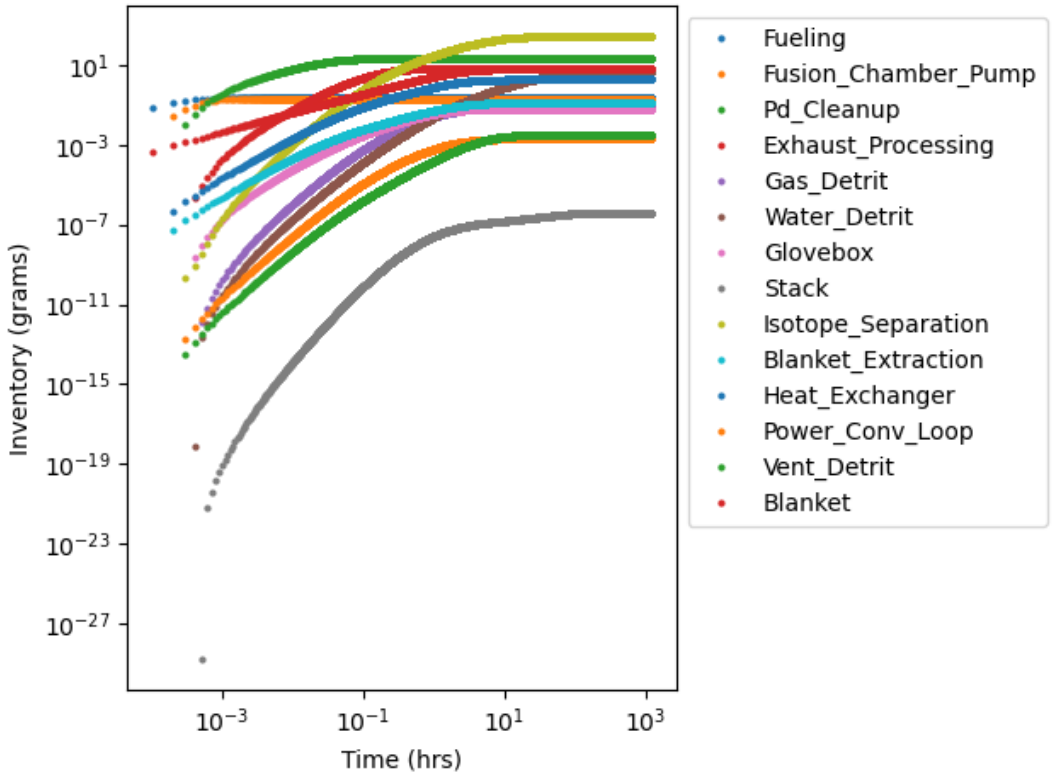

Figure 10. Time dependent inventory of each subsystem in the LLE design over a 50-day period.

B. Li Design Data Plots

Figure 11 shows the time dependent inventory for all subsystems in the Li design and the point at which they reach a steady state inventory. In the case of the Li blanket, a majority of the hydrogen and its isotopes are gettered into the blanket material.

Figure 12 shows the time dependent inventory in storage and delivery over a range of twelve TBR values from 1.25 to 1.85. The curves in the figure demonstrate that TBR does not have a significant impact on the startup inventory (SI). This is because the amount of tritium needed to fill the

processing systems and overcome radioactive decay and stack losses is greater than the amount bred. Once all the processing systems have reached near steady state inventories, the minimum, the amount bred must be greater than the amount lost due to radioactive decay and stack losses. All of the systems with TBR values from 1.25 to 1.85 have an increasing inventory in storage and delivery, meaning that they are more than sufficient to overcome the radioactive decay and stack losses. As the TBR increases the amount bred increases, returning more tritium to storage and delivery; therefore, changes in TBR have a direct impact on the plant doubling time. The higher the TBR the lower the plant doubling time.

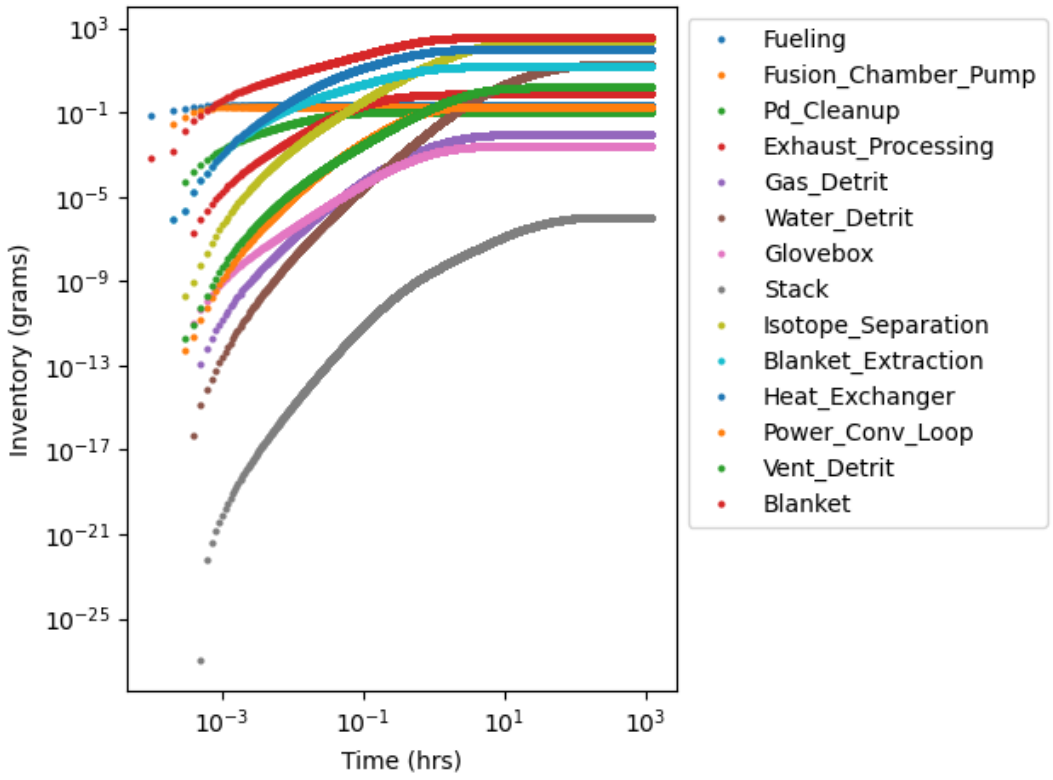

Figure 11. Time dependent inventory of each subsystem in the Li design over a 50-day period.

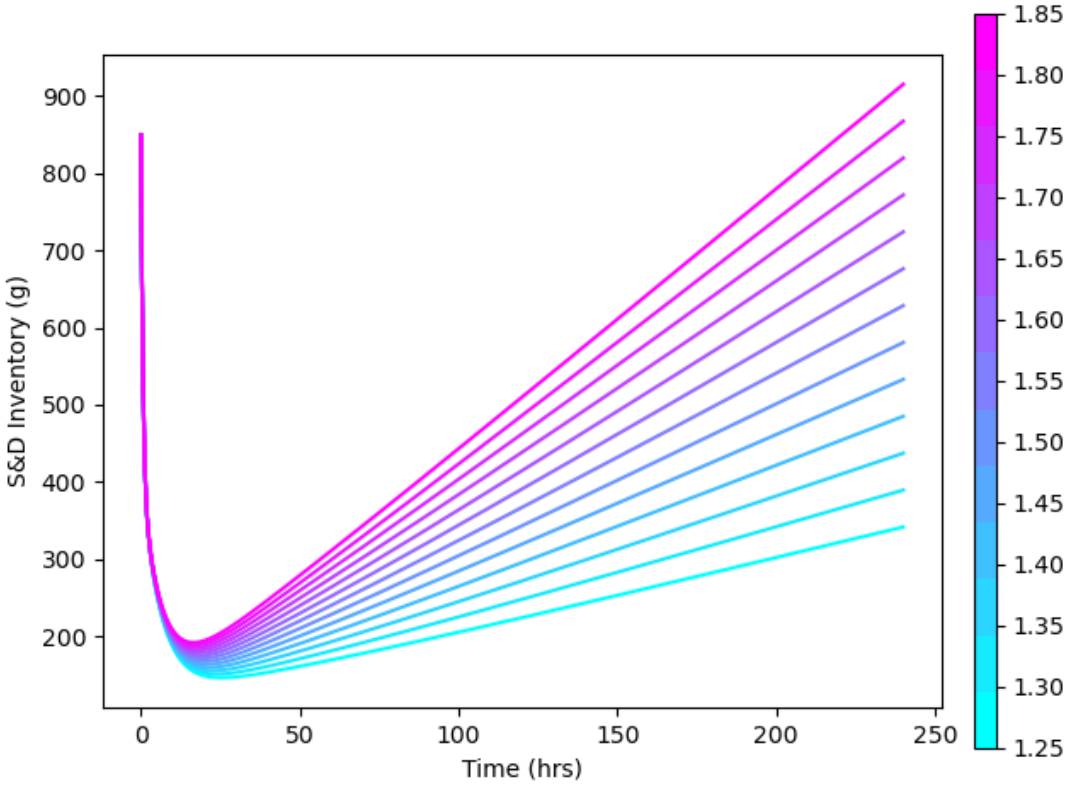

Figure 12. Time dependent inventory in the Storage and Delivery subsystem over a range of 12 TBR values from 1.25 to 1.85 at 0.05 increments.

Appendix 3: Technology Descriptions

A. Megawatt Thermal

The fusion reaction can be described by Equation 4, and 5:

$$^{2}_{1}H \quad + \quad ^{3}_{1}H \quad \rightarrow \quad ^{4}_{2}He \quad + \quad n \qquad \text{Equation 4}$$

$$2.01410178\ amu + 3.01604927\ amu \rightarrow 4.00260325\ amu + 1.00866492\ amu \qquad \text{Equation 5}$$

Equation 5 shows the amount of reactants needed for a single fusion reaction. A single fusion reaction releases 17.589 MeV. The below calculation shows how the tritium ($^{3}_{1}H$) amu, or the amount of reactant in grams per mole, is converted into grams per MW-day. This value is then used to calculate the rough MW_{th} of each GF design.

$$\frac{17.589\ MeV}{3.016604927\ amu} = \frac{17.589\ MeV\ mol}{3.01660497\ gram} \approx 5.8307 \frac{MeV\ mol}{gram}$$

$$\left(5.8307 \frac{MeV\ mol}{gram}\right)\left(6.022 \times 10^{23} \frac{atoms}{mol}\right)\left(\frac{1.066 \times 10^{-19}\left(\frac{MJ}{MeV}\right)}{0.001 \frac{g}{kg}}\right) \approx 562{,}504{,}459.1636 \frac{MJ}{kg}$$

$$\left(1.7779 \times 10^{-9} \frac{kg}{MJ}\right)\left(\frac{1\ MJ}{0.000278\ MW - hrs}\right)\left(\frac{24\ hrs}{1\ day}\right)\left(\frac{1000\ grams}{1\ kg}\right) \approx 0.1535 \frac{grams}{MW - day}$$

$$\text{GF LLE: } \left(\frac{0.1535\ grams}{MW\text{-}day}\right)(500\ MW_{th}) \approx 77\ \frac{grams\ of\ T}{day}$$

$$\text{GF Li : } \left(\frac{0.1535\ grams}{MW\text{-}day}\right)(625\ MW_{th}) \approx 96\ \frac{grams\ of\ T}{day}$$

B. Processing Time of (3) Pd Cleanup

The processing time for the Pd Cleanup was calculated using three inside-out palladium diffusors and four buffer tanks. The sizing of each system is detailed in Figure 13, not to scale, along with the flow rate into the Pd Cleanup subsystem, $0.1797\ \frac{m^3}{min}$, calculated from ASPEN Plus. This value was calculated for the LLE design and it should be noted that there will be a lower flow rate ($0.0045\ \frac{m^3}{min}$) for the Li design blanket due to the Li blanket material acting like a getter for all of the isotopes of hydrogen. This should reduce the size of the Pd Cleanup at the Fusion Chamber and Pump due to the reduced flow rate. This will also impact the processing time of the system.

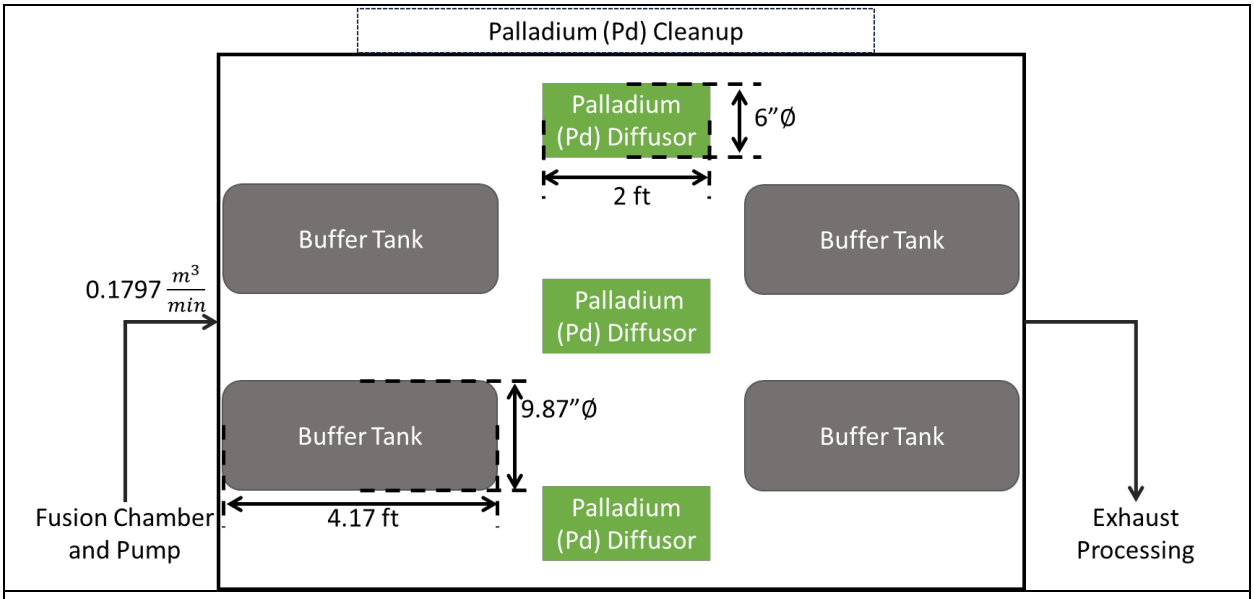

Figure 13. Estimated Pd Cleanup volume for the LLE design.

C. Processing Time of Heat Exchanger

$$Q = \dot{m} * Cp * \Delta T$$

Energy required to change a specific material's temperature dependent on mass flow rate, specific heat capacity, and temperature difference.

$$\Delta T1 = T_{h,in} - T_{c,out}$$

Temperature difference at heat exchanger hot fluid inlet side.

$$\Delta T2 = T_{h,out} - T_{c,in}$$

Temperature difference at heat exchanger hot fluid outlet side.

$$\Delta Tlm = \frac{\Delta T1 - \Delta T2}{\ln\left(\frac{\Delta T1}{\Delta T2}\right)}$$

Log mean temperature difference in a counter current heat exchanger.

$$\mathrm{Q} = \mathrm{U} * \mathrm{A} * \Delta Tlm \qquad \mathrm{A} = \frac{Q}{U * \Delta Tlm}$$

Total energy transfer in a counter current heat exchanger based on the overall heat transfer coefficient of the heat exchanger, total surface area for heat transfer, and the log mean temperature difference. The second equation is rearranged to solve for required surface area of the heat exchanger as that is what we are interested in.

For the purposes of these calculations a U value of 400 W/m^2*K was assumed that is typical for a system with high pressure gas and a liquid as the heat transfer fluids.

1. LLE Design Heat Exchanger

$$Q = 10500\left[\frac{kg}{s}\right] * 188.6\left[\frac{J}{kg * K}\right] * (823.15\,K - 573.15K) = 495124350\,\mathrm{W} = 495124\,\mathrm{kW}$$

$$\Delta T1 = 550C - 500\mathrm{C} = 50\mathrm{C}$$

$$\Delta T2 = 300C - 20\mathrm{C} = 280\mathrm{C}$$

$$\Delta Tlm = \frac{50 - 280}{\ln\left(\frac{50}{280}\right)} = 133.5\,K$$

$$\mathrm{A} = \frac{495124350\,W}{400\left[\frac{\mathrm{W}}{m^2 * K}\right] * 133.5\,K} = 9271.5\,m^2$$

2. Li Design Heat Exchanger

$$Q = 1000\frac{kg}{s} * 4169\frac{J}{kg * K} * (823.15\,K - 493.15K) = 1.375e10^9 W = 1375770\,kW$$

$$\Delta T1 = 550C - 500\mathrm{C} = 50\mathrm{C}$$

$$\Delta T2 = 220C - 20\mathrm{C} = 200\mathrm{C}$$

$$\Delta Tlm = \frac{50 - 200}{\ln\left(\frac{50}{200}\right)} = 108.2\,K$$

$$\mathrm{A} = \frac{1.375e10^9 W}{400\left[\frac{\mathrm{W}}{m^2 * K}\right] * 108.2\,K} = 31787\,m^2$$

Using the required surface area for total energy transfer between the two fluids calculated above assuming a single pass counter-current heat exchanger, the total volume of the heat exchanger's

tubes can be calculated. This requires knowing the diameter of the tubes and the number of tubes necessary to achieve the desired surface area before translating those values into a volume which gets into the realm of full heat exchanger design. Due to the arbitrary nature of choosing values to calculate the total volume, a reasonable volume of 100 cubic meters was chosen for both systems for direct comparison.

With that being said, the amount of energy necessary to remove from the lithium blanket is very high and the temperature difference is the main culprit of this value. It would most likely be necessary to utilize a series of heat exchangers to handle the full load of such a large temperature swing. This would increase blanket residence time, thus increasing the inventory of tritium in the system. The large temperature swing would also require vast quantities of cooling fluid to achieve such a change, further increasing operating and capital costs of the system.

D. Volume of Blanket outside of Fusion Chamber

The volume of blanket material held up in piping will be largely tied to the diameter of the pipe being utilized in the fusion facility which will ultimately be limited by the velocity the blanket material can be reasonably moved at. If a reasonable value for the blanket material's velocity is determined, the pipe volume necessary can easily be determined based on the volumetric flowrate of 2 m^3/s by choosing a pipe diameter.

$$Cross\ Sectional\ Area\ of\ a\ Circle = \ A = \pi r^2$$

Due to the volumetric flowrate being 2 m^3/s achieving a blanket velocity of even 2.5 m/s would require a pipe with a diameter of approximately 1 meter (A = 0.8 m^2), which would very quickly scale the required volume of blanket material.

If we assume this is achievable with about 100 meters of pipe and account for the volume of blanket material in the chamber (V = 329 m^3), piping (V ≈ 80 m^3), heat exchanger (V ≈ 100 m^3), and the blanket detritiation system (V ≈ 5 m^3), the approximate total volume of blanket material needed would be on the order of 500 m^3 on the low end and could approach 1000 m^3 as a high end conservative estimate.

Bibliography & References Cited

1. Laboratories, C.N., *Tritium Removal from Molten Breeder in the General Fusion*. 2022.
2. Abdou, M.A., et al., *Deuterium-Tritium Fuel Self-Sufficiency in Fusion Reactors.* Fusion Technology, 1986. **9**(2): p. 250-285.
3. Flynn, H.B. and G. Larsen, *Investigating the application of Kalman Filters for real-time accountancy in fusion fuel cycles.* Fusion Engineering and Design, 2022. **176**: p. 113037.
4. Flynn, H.B. and G. Larsen, *Fusion Fuel Cycle Inventory Reduction Studies Using a Processing-Time–Based Discrete-Time Interval Model.* Fusion Science and Technology, 2022. **79**(1): p. 60-68.
5. Teprovich, J.A., et al., *Electrochemical extraction of hydrogen isotopes from Li/LiT mixtures.* Fusion Engineering and Design, 2019. **139**: p. 1-6.

6. Maroni, V.A., R.D. Wolson, and G.E. Staahl, *Some Preliminary Considerations of A Molten-Salt Extraction Process to Remove Tritium from Liquid Lithium Fusion Reactor Blankets.* Nuclear Technology, 2017. **25**(1): p. 83-91.
7. Collin R Malone, H.B.F., Alex D Somers, P Arron Rowell, George K Larsen, *Approach to Startup Inventory for Viable Commercial Fusion Power Plant* 2024.
8. Stubbers, R., et al., *Measurement of hydrogen absorption in flowing liquid lithium in the flowing lithium retention experiment (FLIRE).* Journal of Nuclear Materials, 2005. **337-339**: p. 1033-1037.
9. Baldwin, M.J., et al., *Plasma interaction with liquid lithium: Measurements of retention and erosion.* Fusion Engineering and Design, 2002. **61-62**: p. 231-236.
10. Meschini, S., et al., *Modeling and analysis of the tritium fuel cycle for ARC- and STEP-class D-T fusion power plants.* Nuclear Fusion, 2023. **63**(12).
11. Glugla, M., et al., *The ITER tritium systems.* Fusion Engineering and Design, 2007. **82**(5-14): p. 472-487.
12. Pearson, R.J., A.B. Antoniazzi, and W.J. Nuttall, *Tritium supply and use: a key issue for the development of nuclear fusion energy.* Fusion Engineering and Design, 2018. **136**: p. 1140-1148.
13. Commission, U.S.N.R. *Code of Federal Regulations (CFR), Title 10, 20.1301(a)(1)*. Available from: https://www.ecfr.gov/current/title-10/chapter-I/part-20/subpart-D/section-20.1301.
14. Humrickhouse, P.W., J.P. Sharpe, and M.L. Corradini, *Comparison of hyperelastic models for granular materials.* Phys Rev E Stat Nonlin Soft Matter Phys, 2010. **81**(1 Pt 1): p. 011303.
15. Liu, L., et al., *Analysis of the whole process tritium transport based on fuel cycle modeling for CFETR.* Fusion Engineering and Design, 2020. **161**: p. 112060.
16. Abdou, M., et al., *Physics and technology considerations for the deuterium–tritium fuel cycle and conditions for tritium fuel self sufficiency.* Nuclear Fusion, 2020. **61**(1): p. 013001.
17. Day, C. and T. Giegerich, *The Direct Internal Recycling concept to simplify the fuel cycle of a fusion power plant.* Fusion Engineering and Design, 2013. **88**(6-8): p. 616-620.
18. Wilson, J., et al., *The ITER Tokamak Exhaust Processing System Permeator and Palladium Membrane Reactor Design.* Fusion Science and Technology, 2019. **75**(8): p. 802-809.